Submitted to small

DOI: 10.1002/smll.((please add manuscript number))

# Flexible, transparent, conducting films of randomly stacked graphene from surfactant-stabilised, oxide-free graphene dispersions

*Sukanta De, Paul J King, Mustafa Lotya, Arlene O'Neill, Evelyn M Doherty, Yenny Hernandez, Georg S Duesberg, and Jonathan N Coleman**

[*] Prof. J. N. Coleman, Dr. S. De, P. J. King, M. Lotya, A. O'Neill, E. M. Doherty, Dr. Y. Hernandez

School of Physics,

Centre for Research on Adaptive Nanostructures & Nanodevices (CRANN),

Trinity College Dublin, University of Dublin,

Dublin 2 (Ireland).

E-mail: colemaj@tcd.ie

Prof. G. S. Duesberg

School of Chemistry,

Centre for Research on Adaptive Nanostructures & Nanodevices (CRANN),

Trinity College Dublin, University of Dublin,

Dublin 2 (Ireland).

Keywords: Graphene, Transparent conducting film, Electron microscopy, Conductivity

We have exfoliated graphite in water to give dispersions of mono and few-layer graphene stabilised by surfactant. These dispersions can be used to form thin, disordered films of randomly stacked, oxide-free, few-layer graphenes. These films are transparent with a DC conductivity of up to $1.5\times10^4$ S/m. The conductivity is stable under flexing for at least 2000 cycles. The electrical properties are limited by disorder and aggregation suggesting future routes for improvement.

## 1. Introduction

Transparent conductors are an extremely important component of modern technology. The most commonly used materials are doped metal oxides such as indium tin oxide (ITO). However, the future of ITO as the main material in this area may be limited for economic and technical reasons[1, 2]. In short, a new material is required which must be compatible with low temperature, large area deposition and must be flexible. This is in addition to displaying high transparency, T, and low sheet resistance, $R_s$, associated with ITO.

Over the last decade, a number of materials have been proposed. These range from thin films of common metals[3, 4] or metal grids[5] through conducting polymer films[6] to networks of metal nanowires[7, 8]. A large number of reports have appeared describing nanotube films as transparent conductors.[1, 9-19] To date, nanotube films have been prepared with DC conductivities close to $6\times10^5$ S/m.[14, 19] This value is important because, it represents the threshold, above which in principle (see below), films can be prepared with T>90% for $R_s$<100 Ω/ .[2] These are the minimum standards required for a material to be industrially useful as a transparent conductor. In addition, nanotube films[2] and polymer-nanotube composite films[1] have been shown to be electrically stable under flexing. However, while attractive, nanotubes are still very expensive. Arc-discharge SWNT which are known to form the most conductive films cost approximately $1500/g (Iljin Nanotech)[2]. By contrast, the graphite powder used in this work costs ~$5/kg.

An alternative solution would be the identification of a cheaper, alternative form of graphitic nano-carbon which can be formed into highly conductive, thin, transparent films. We believe that thin films of layered (but not Bernal, i.e. AB, stacked) graphene are such a material. Graphene is a monolayer of $sp^2$ bonded carbon and is generally found stacked together in the form of graphite[20]. While graphene displays huge potential, large scale

exfoliation of graphite to give graphene was long considered impossible. To get around this, researchers have developed methods to heavily oxidise graphite in acid to give graphite oxide[21]. This can then be exfoliated in water to give dispersions of graphene oxide which can be used to form composites[22] or films[23]. While themselves insulating, these films can be reduced either thermally or using chemicals such as hydrazine to give a material that approaches graphene[21]. However, we emphasize that such chemically modified graphene (CMG) always contains residual oxides[24, 25] as demonstrated by FTIR, XPS and structural defects as shown by Raman spectroscopy[21]. While CMG is conductive, its electronic properties deviate significantly from those of pristine graphene.

CMG has been used by a number of groups to produce thin, transparent, conducting films [24, 26-30].The most conductive of these films have displayed DC conductivities between $10^4$ and $10^5$ S/m.[27, 29, 30] However, such films have required thermal annealing at 1100$^o$C to achieve these conductivities. Such temperatures are prohibitive for many applications and completely rule out any role in plastic electronics. By contrast Eda et al described annealing at only 200$^o$C but achieved DC conductivity of <1000 S/m.[28]

Avoidance of this high temperature processing has become conceivable following breakthroughs which allow the liquid phase exfoliation of graphite to give dispersions of defect-free graphene. This exfoliation can be achieved in certain organic solvents[31, 32] or in water-surfactant solutions[33]. These graphene-rich dispersions can be used to form films. As neither oxides nor structural defects are created during the exfoliation process, in principle thin conducting films can be produced without high temperature annealing or chemical reduction. In this work we have used surfactant stabilized dispersions of graphene in water to prepare a range of thin films with varying thickness. We have characterized these films using microscopy and spectroscopy as well as measuring the DC conductivity. We find

conductivities of up to ~$10^4$ S/m coupled with optical transmittance of up to 90%. In addition these films are electromechanically stable under bending for at least 2000 cycles.

## 2. Results and Discussions

The key to this work is the ability to exfoliate graphite to give graphene in the liquid phase without any oxidisation or significant defect formation. We employ the simple approach of sonicating the graphite powder in a solution of the surfactant sodium cholate in water to give dark coloured dispersions (figure 1A). Sodium cholate is well known as an efficient surfactant for carbon nanotubes[34, 35]. After centrifugation, we get grey dispersions with concentration as high as 0.04 mg/ml but typically ~0.005 mg/ml (figure 1A). This procedure is similar to the one previously outlined for graphite exfoliation using sodium dodecyl benzene sulfonate[33]. However, we believe sodium cholate to be a far superior surfactant in terms of the concentration and the degree of exfoliation achievable. TEM analysis[31] of the dispersions after centrifugation show large quantities of mono- and few-layer graphenes (figure 1 B, C). We note that these flakes tend to be folded more than those observed for solvent exfoliated graphene[31]. The high degree of exfoliation achievable in these dispersions makes them ideal for applications such as the preparation of thin conducting films.

We have prepared thin graphitic films by vacuum filtration of these graphene-rich, surfactant-stabilised dispersions[33]. Shown in figure 2A and B are photographs of as-prepared thin graphitic films (TGFs) with average thicknesses of t=6 nm and t=40 nm respectively. These films are optically uniform; the spatial non-uniformity of the transmittance was $\Delta T/T<4\%$ (standard deviation of local transmission measured over 500×500 4 μm sized pixels / mean transmission). We investigate the film surface (t=72 nm) more closely using scanning

electron microscopy as shown in figure 2 C. It is clear from this image that these films consist of a disordered array of graphitic flakes lying approximately in the plane of the film. These flakes range in lateral size from ~100 nm to ~3 μm. While it is impossible to gauge their thickness from these images, a number of the flakes appear significantly thicker than monolayers suggesting that some aggregation of the graphene flakes has occurred during film formation. However, some flakes appear partially transparent to the electron beam, suggesting them to be relatively thin.

It is important to note that we prepare these films from dispersions of graphene[33] not graphene oxide; measurements have shown this type of dispersion process does not introduce significant quantities of defects or oxides to the flakes[31, 33]. Nevertheless, it is important to confirm the absence of defects or oxides in these filtered films. We test for oxides using FTIR as shown in figure 2E. Oxides such as C=O, -COOH or C-O groups have characteristic features at 1000 $cm^{-1}$ and 1700 $cm^{-1}$ respectively. These features tend to be relatively intense in FTIR spectra of graphene oxide films[24]. No such features are observed here. We note that the features appearing in figure 2E in the range 600-1300 $cm^{-1}$ are associated with the glass substrate.

We can also test for the presence of structural defects using Raman spectroscopy. Shown in figure 2F is a Raman spectrum (633 nm) for an as-produced film with the spectrum of the starting graphite powder shown for comparison. Three bands are immediately clear; the D band around 1300 $cm^{-1}$, the G band around 1600 $cm^{-1}$ and the 2D band around 2650 $cm^{-1}$. Of most interest are the D and 2D bands. The D band is indicative of the presence of defects, which in graphene are generally divided into basal plane defects and edge defects. Previous studies of graphene exfoliated from graphite using surfactants[33] or amide solvents[31] have shown very small D bands which have been attributed to flake edges. In the thin film shown here, this band is relatively intense compared to the smaller band observed in the graphite

powder. (In addition the growth of the shoulder at ~1615 $cm^{-1}$ is indicative of some defect creation.[36]) At first sight this suggests the presence of basal plane defects, possibly induced during sonication. However, it more probably reflects the formation of new edges as flakes are cut during sonication. In addition, we note that this band is much narrower than those typically observed for defective CMGs[21]. Thus, while edge defects may be introduced during sonication, the basal defect content should be much lower than that found in chemically modified graphenes. We can also look at the 2D band. The shape of this band is indicative of the number of monolayers per flake[37]. We note that the shape of this band for the as-produced film is significantly different to the 2D band of graphite and is reminiscent of few layer graphene[37]. This would suggest that although aggregation occurs during film formation, the aggregates are not Bernal stacked but rather are randomly re-stacked. As such the films are neither graphite nor graphene but a disordered array of few-layer graphenes, perhaps are best classified as randomly restacked graphene.

We have measured the optical and electrical properties of these as-produced graphitic films. Shown in figure 3A are optical transmission spectra for a range of films with varying thickness. These spectra are broad and featureless as expected for a material composed of 2-dimensional entities. Typically the transmittance varies from ~90% to ~35% as the thickness increases from 6 nm to 88 nm. We have measured the sheet resistance of the films to fall from $10^6$ Ω/ to $10^3$ Ω/ over the same range. The transmittance (550 nm) is plotted as a function of sheet resistance in figure 3B. Here, both transmittance and sheet resistance fall off as the film thickness increases.

In general for thin metallic films, the transmittance is related to the sheet resistance by[38, 39]:

$$T = \left(1 + \frac{Z_0}{2R_s}\frac{\sigma_{Op}}{\sigma_{DC}}\right)^{-2} \quad \text{equation 1}$$

where $Z_0$=377 Ω is the impedance of free space and $\sigma_{DC}$ and $\sigma_{Op}$ are the DC and optical conductivity respectively. This expression can be fitted to the data in figure 3B with a good fit obtained for films with t>20 nm (deposited mass per area M/A>40 mg/m$^2$). This fit gives a value of $\sigma_{DC}/\sigma_{Op}$ ~0.04 for the as-prepared films.

One can use equation 1 to estimate $\sigma_{DC}/\sigma_{Op}$ from the data presented in the literature for transparent films based on CMG. In all cases these films were reduced thermally with $\sigma_{DC}/\sigma_{Op}$ increasing with anneal temperature. For example, Eda et al produced films from hydrazine reduced CMG which had been annealed at 200C. These films had $R_s$~$10^5$ Ω/ @ T~85% giving $\sigma_{DC}/\sigma_{Op}$ = 0.02.[28] Li et al[24] exfoliated graphite with the aid of acid allowing them to prepare films by the LB technique. These are annealed at 800$^o$C to remove oxides, resulting in films with $\sigma_{DC}/\sigma_{Op}$ ~0.2 ($R_s$~$10^4$ Ω/ @ T~80%). Wu et al[30] spun cast CMG to produce films which were subsequently annealed at 1100$^o$C to give $\sigma_{DC}/\sigma_{Op}$ ~0.5 ($R_s$~3500 Ω/ @ T~82%). Wang et al*[29]* prepared films of CMG by dip-coating followed by annealing at 1100$^o$C with $\sigma_{DC}/\sigma_{Op}$ ~0.42 ($R_s$~1800 Ω/ @ T~64% at 550 nm (quoted data: 70% at 1000 nm)). Similarly Becerril[27] et al produced CMG films by spin coating. By using a combination of hydrazine reduction and annealing at 400$^o$C they achieved $R_s$~$10^4$ Ω/ @ T~60%, resulting in $\sigma_{DC}/\sigma_{Op}$ ~0.06. By annealing at 1100$^o$C they produced films with $R_s$~330 Ω/ @ T~60%, resulting in $\sigma_{DC}/\sigma_{Op}$ ~2. For comparison purposes, this data is summarised in figure 3 (inset). This makes clear that the annealed films quoted in the literature out-perform our as-produced graphitic films. We must consider a post-treatment technique to improve the properties.

While we have shown that our graphitic films have low defect contents compared to CMGs, it may be advantageous to perform an annealing step. There are two reasons for this; micromechanically cleaved graphene is generally annealed to improve electrical

performance[20] and by analogy with nanotube films, a post-treatment may remove residual surfactant[15]. We annealed a number of films (t=40nm) in flowing $H_2$/Ar at a range of temperatures from 200°C to 1000°C. SEM analysis (figure 2D) shows no significant difference in film morphology before and after annealing at 500°C. In addition FTIR and Raman analysis (figure 2E and F) show no change in oxide or defect content. We measured $R_s$ and T for all annealed films, using the data to calculate $\sigma_{DC}/\sigma_{Op}$. As shown in fig 3B, inset, the measured value of $\sigma_{DC}/\sigma_{Op}$ is constant below 200°C but increases dramatically between 200°C and 500°C before levelling off above 500°C at $\sigma_{DC}/\sigma_{Op}$~0.35. We note from this data that our graphitic films out-perform the reduced CMG films at all anneal temperatures below 1100°C. We then prepared films with a range of thickness, before annealing at 500°C. The transmittances and sheet resistances are shown in figure 3B. The data fits well to equation 1 for t>20 nm with the fit giving $\sigma_{DC}/\sigma_{Op}$ ~0.4. We note that while $\sigma_{DC}/\sigma_{Op}$ ~0.4 is close to the state of the art for thin films prepared from CMG, it is a long way from industrial requirements. The minimum industry standards for a transparent conductor are T>90% for $R_s$<100 Ω/ . This means the minimum acceptable value of the conductivity ratio is $\sigma_{DC}/\sigma_{Op}$ =35. Below, we will discuss methods to bridge this gap.

To complete our analysis we measured the thickness dependence of the film properties for films annealed at 500°C (see SI for description of film thickness measurement). We measured T (550 nm) and $R_s$ as shown in figure 4A and B. Note the data for un-annealed films are shown for comparison. As t is increased, T decreases smoothly for both film types. For thin conducting films, the transmittance scales with thickness as[39]:

$$T = \left(1 + \frac{Z_0}{2}\sigma_{Op} t\right)^{-2} \quad \text{equation 2}$$

This expression can be well fitted to both data sets with a value of $\sigma_{Op} \approx 4.2 \times 10^4$ S/m. When one analyses data presented in the literature for reduced CMG films, one finds values of $\sigma_{Op}$

in the range 5-10×$10^4$ S/m, in reasonable agreement with our value[27-29]. We note that when analysed using equation 2, Nair's transmittance data for micromechanically cleaved graphene suggests $\sigma_{Op}$=1.8×$10^5$ S/m.[40] We suggest that the lower value recorded here reflects the different inter-layer interactions associated with randomly restacked graphene. Shown in figure 4B is data for $R_s$ for each film type. While both data sets decrease with increasing film thickness, the annealed data is significantly lower than the as-produced. In addition while both data sets scale inversely with thickness at high thicknesses, both sets display anomalously high sheet resistances at lower film thickness. This effect has been observed for films of both carbon nanotubes[2] and silver nanowires[8].

To see this more clearly we calculate the DC conductivity from $\sigma=1/R_s t$, as shown in figure 4C. Note that the conductivity ratio, $\sigma_{DC}/\sigma_{Op}$, is shown on the right axis. For both film types the DC conductivity is constant for thicknesses above 20 nm. For the annealed film, $\sigma_{DC}$=1.5×$10^4$ S/m above 20 nm ($\sigma_{DC}/\sigma_{Op}$~0.4). Such a DC conductivity value is close to the best data for chemically modified graphene films[41]. However for thinner films the conductivity falls off significantly. Such behaviour is observed for other nano-structured thin films[1, 2, 8, 14] and has previously been attributed to thickness non-uniformity at low thickness[2, 8]. To study this, we measure the film thickness non-uniformity by measuring the spatially resolved absorbance using a transmission scanner[2, 8]. We define the non-uniformity as the standard deviation of absorbance divided by the mean absorbance, ΔA/A. We plot this parameter for both film types in figure 4D. In both cases, the non-uniformity is constant for thicknesses above 20 nm. However below t=20 nm the non-uniformity increases substantially. We suggest that it is this increased non-uniformity which causes the reduction in conductivity at low thicknesses. For nanotube and nanowire films, it has been suggested that the increase in non-uniformity tends to occur for thicknesses close to twice the nanotube bundle / nanowire diameter[2, 8]. If a similar rule applied here, it would suggest that the graphitic flakes making

up the films are typically ~10 nm in thickness. This suggests significant aggregation has occurred during film formation.

We note that the uniformity is better in the annealed samples. To test this further we performed atomic force microscopy on a number of our films (see supporting information). Such images showed graphitic flakes of sizes similar to those in the SEM images. These flakes displayed a range of heights from a few nm to 10s of nm. We measured the root mean square roughness for films before and after annealing finding values of ~13 nm and ~11 nm respectively. The films after annealing were consistently about 20% less rough suggesting that some re-organisation occurs during annealing.

Nano-structured, thin, transparent films are most likely to be used in e-paper type applications. Thus they must retain their conductivity under flexing. We monitored the film conductivity under both tensile and compressive bending for two graphitic films on PET of thickness 40 nm and 88 nm as shown in figure 5. During the first bend cycle (insets) the resistance increased slightly for the films in tension. The compressively bent films displayed more complex behaviour but varied by no more than 6% from the initial resistance. We also plot the mean sheet resistance per cycle for both films. In each case the resistance falls slightly over 2000 cycles. We note that none of the films failed. Rather the measurement was limited by time constraints.

## 3. Conclusion

We have demonstrated the preparation of thin transparent films of graphene. The electrical stability coupled with the high levels of transparency observed and the low cost of graphite make these films attractive as transparent conductors. However, like CMG based films, these films have DC conductivity much too low for practical purposes. In addition, the

need to anneal is a big disadvantage. However, they do have some significant advantages over CMG based films. Most importantly, the flakes are graphene at all stages, there is no need to oxidise or reduce. Because of this, the requirement to anneal is not intrinsic. We suspect it aids removal of residual surfactant and facilitates some rearrangement of graphene sheets. We believe that such effects can be achieved by improving the dispersion or film formation process, perhaps by washing or acid treatment (mild enough not to oxidise the graphene). In addition, these films have much lower defect contents compared to CMG films. This means the ultimate conductivity of these films is likely to be much higher. Finally, these films consist of large aggregates which contribute to roughness and provide the ultimate limit to conductivity. Improvements in the dispersion or film formation procedures will reduce this aggregation leading to better quality films with much higher DC conductivities. In contrast CMG films display much less aggregation. This means they have much less scope for improvement. We believe further improvement is possible which could see these films supersede carbon nanotube films as the heirs to ITO.

**4. Experimental Section**

Graphite was purchased from Branwell Graphite Ltd (Branwell natural graphite, grade 2369, www.branwell.u-net.com/, typical cost $5/kg) while sodium cholate surfactant was purchased from Aldrich. Both products were used as supplied. A stock solution of sodium cholate (SC) (5mg/ml) was prepared by stirring overnight in Millipore water. This was subsequently diluted for further use. Graphite (initial concentration 0.75mg/ml) was dispersed in 25 ml SC solution (concentration 0.5mg/ml) by sonication for 140 mins in a low power ultrasonic bath (Branson 1510E-MT bath sonicator). The resulting dispersion was left to stand for 24hrs to allow any unstable aggregates to form. The top 80% of the dispersion was decanted and discarded. SC was then added to maintain the starting volume of dispersion at

25ml. This was then sonicated for a further 140mins. Again the dispersion was left to stand overnight and then centrifuged at 5000rpm for 90min (Hettich Mikro 22R). After centrifugation the top 80% of supernatant was decanted and retained for use. The post centrifuge graphene concentration was estimated from absorbance measurements (Varian Cary6000i) using the measured extinction coefficient of graphene in surfactant water solutions (1390 ml $mg^{-1}$ $m^{-1}$)[33].

The resulting dispersions were vacuum filtered using porous cellulose filter membranes (MF-Millipore membrane, mixed cellulose esters, hydrophilic, 0.025µm 47 mm) to give thin graphitic films. The thickness of these films was controlled by the volume of dispersion filtered, and hence the deposited graphene mass. The deposited films were then transferred onto glass slides using iso-propanol to remove trapped air between the film and substrate thus improving adhesion. The cellulose filter membrane was then removed by treatment with acetone vapour and subsequent acetone liquid baths followed by a methanol bath[19]. The final film diameter was 36 mm. The film thickness, *t*, was measured by AFM (see supporting information). Films were annealed at various temperatures under $H_2$/Ar flow for 2hrs.

Optical transmission spectra were recorded before and after anneal using a Varian Cary 6000i. In all cases, a glass slide was used as the reference. Sheet resistance measurements were made before and after anneal using the four-probe technique with silver electrodes of dimensions and spacings typically of ~mm size and a Keithley 2400 source meter. Transmission scans were made using an Epson Perfection V700 photo flat-bed transmission scanner with a bit depth of 48 bits per pixel and a spatial resolution of 6400 dpi.[2] TEM samples were prepared by pipetting a few milliliters of this dispersion onto holey carbon mesh grids (400 mesh). Bright-field TEM images were taken with a Jeol 2100, operated at 200 kV. Scanning electron microscopy measurements were made using a Zeiss

Ultra plus SEM. Raman spectra were taken on a Horiba Jobin Yvon LabRAM-HR using a 100× objective lens with a 633 nm laser excitation. Attenuated total reflectance FTIR spectra of these films were taken on a Perkin-Elmer Spectrum 100. AFM measurements for surface roughness and thickness were taken with a Digital Instruments Nanoscope IIIA from Veeco Systems in tapping mode using silicon tips with a resonance frequency of 320 kHz. Electromechanical measurements were made using a Zwick Z0.5 Proline tensile tester as described previously[1, 2].

Acknowledgments

The authors acknowledge Science Foundation Ireland through the principle investigators scheme for supporting this work.

Figures

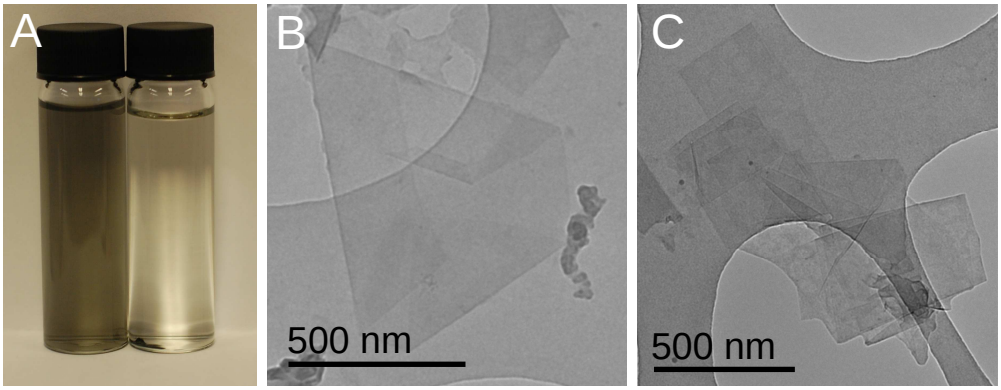


Figure 1: A) Photograph of a water/sodium cholate graphene dispersion before (left) and after (right) centrifugation. B) & C) TEM images of graphene flakes deposited from sodium cholate stabilized aqueous graphene dispersions. A) A folded monalayer. B) An aggregate containing a folded ribbon.

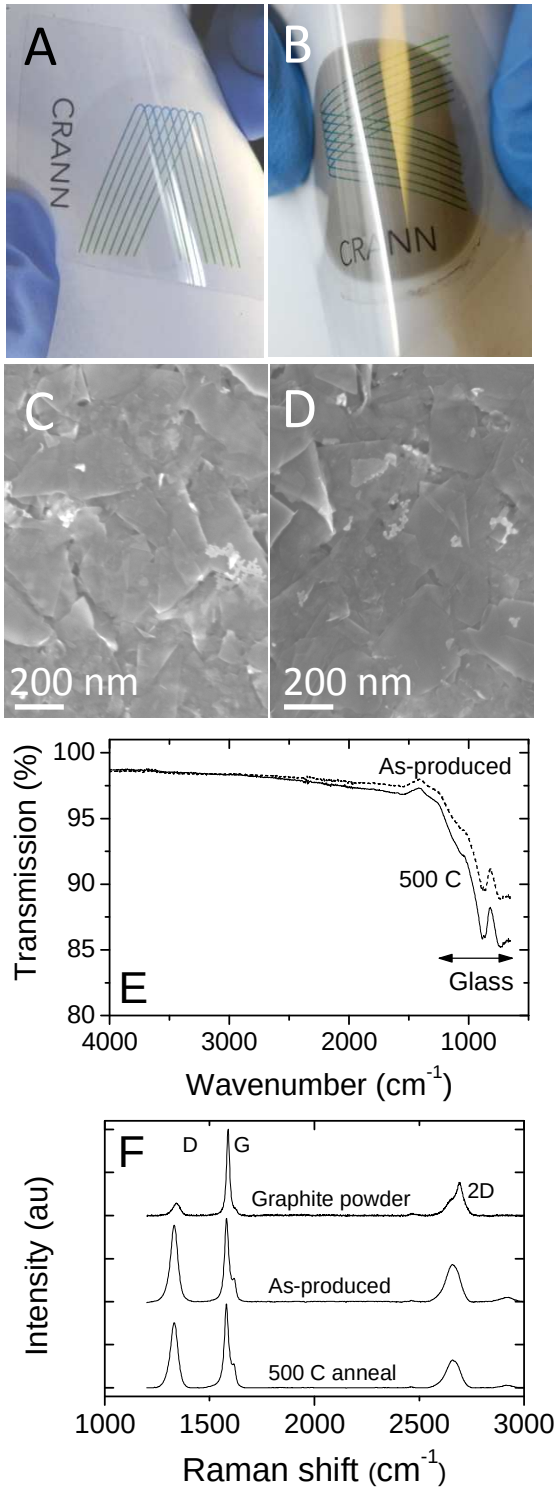


Figure 2: A) and B) Photographs of graphitic films on PET (thicknesses of 6 nm and 40 nm respectively). C) and D) SEM images of 72 nm thick graphitic films before and after annealing at 500 $^{o}$C respectively. E) ATR-FTIR spectra for both as-produced and annealed

graphitic films. Neither spectrum shows any evidence of oxidisation. F) Raman spectra (633 nm) for graphite powder, an as-produced film and an annealed film.

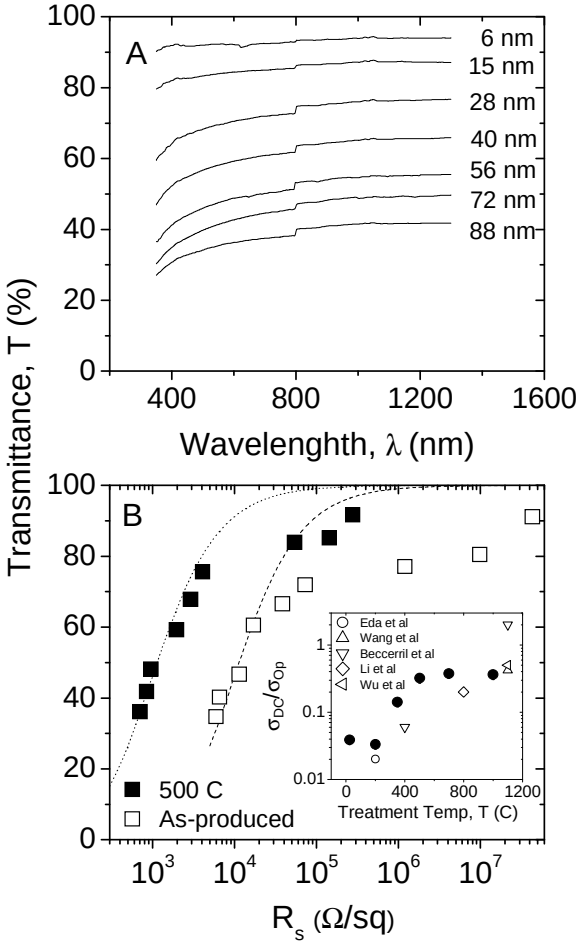


Figure 3: A) Transmittance spectra for thin as-produced graphitic films of various thicknesses. NB the spectra were not altered by annealing. B) Transmittance (550 nm) plotted as a function of sheet resistance for both as-produced and annealed (500C) films. The dashed lines are fits to equation 1 and are defined by $\sigma_{DC}/\sigma_{Op}=0.04$ and $\sigma_{DC}/\sigma_{Op}=0.4$ for as-produced and annealed film respectively.

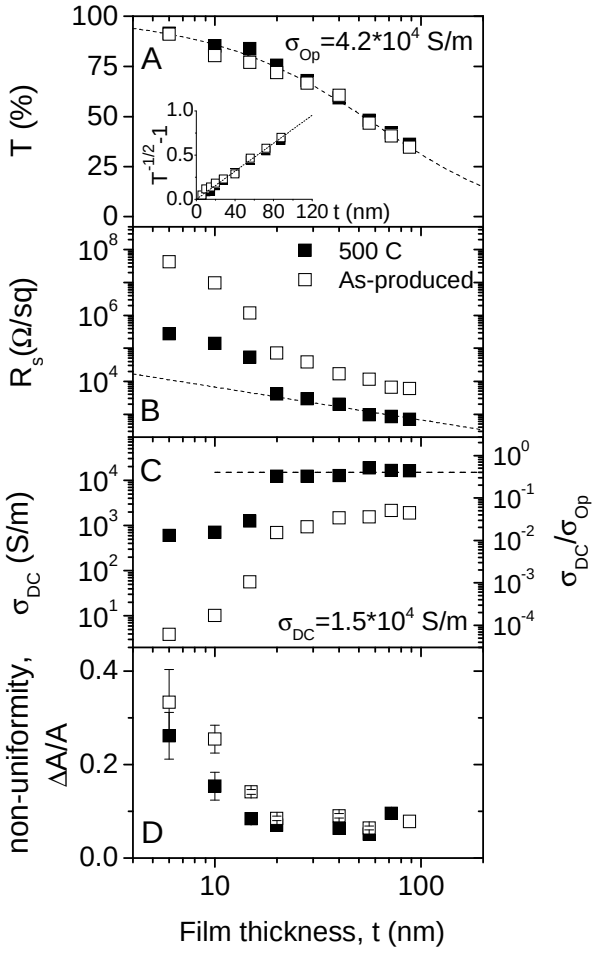


Figure 4: Optical, electrical and uniformity data for as-produced and annealed (500C) films. A) Transmittance (550 nm) plotted as a function of film thickness. The dashed line is a fit to equation 2 and is defined by $\sigma_{Op}=4.2\times10^4$ S/m. Inset: The same data is plotted to illustrate the applicability of equation 2. B) Sheet resistance as a function of thickness. The dashed line illustrates bulk behaviour. C) DC conductivity plotted versus film thickness. Note that the DC conductivity falls off below t=20 nm. The right axis denotes $\sigma_{DC}/\sigma_{Op}$. D) Film non-uniformity plotted versus film thickness. The non-uniformity is defined as the standard deviation of a set of spatially resolved absorbance measurements divided by the mean absorbance.

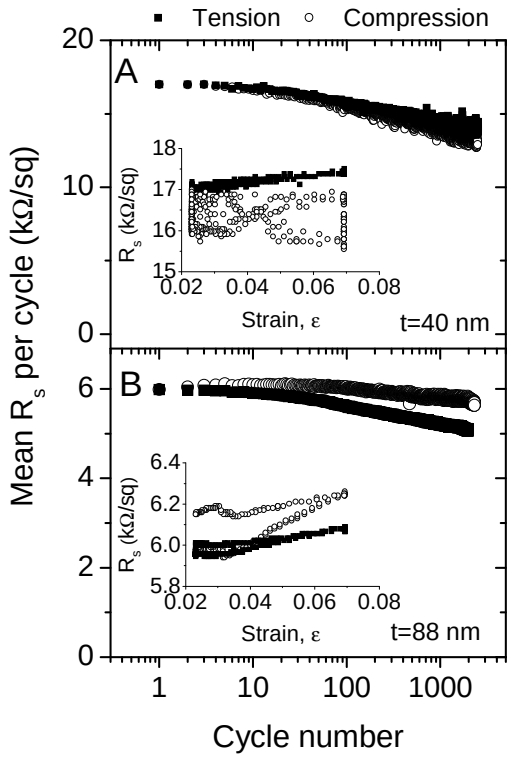


Figure 5: Sheet resistance during bending for as-produced films deposited on PET. Measurements were made for films both in tension and compression. Data for A) a 40 nm thick film and B) an 88 nm thick film. Inset: Resistance versus strain for the first cycle. Main graph: Mean resistance per cycle versus cycle number

References

[1] S. De, P. E. Lyons, S. Sorrel, E. M. Doherty, P. J. King, W. J. Blau, P. N. Nirmalraj, J. J. Boland, V. Scardaci, J. Joimel, J. N. Coleman, *ACS Nano* **2009**, *3*, 714.
[2] E. M. Doherty, S. De, L. Lyons, A. Shmelov, P. N. Nirmalraj, V. Scardaci, W. J. Blau, J. J. Boland, J. N. Coleman, *Carbon* **2009**, *47*, 2466.
[3] J. Meiss, M. K. Riede, K. Leo, *Applied Physics Letters* **2009**, *94*, 013303
[4] B. O'Connor, C. Haughn, K. H. An, K. P. Pipe, M. Shtein, *Applied Physics Letters* **2008**, *93*, 223304.
[5] M. G. Kang, M. S. Kim, J. S. Kim, L. J. Guo, *Advanced Materials* **2008**, *20*, 4408.
[6] Y. H. Zhou, F. L. Zhang, K. Tvingstedt, S. Barrau, F. H. Li, W. J. Tian, O. Inganas, *Applied Physics Letters* **2008**, *92*, 233308.
[7] J. Y. Lee, S. T. Connor, Y. Cui, P. Peumans, *Nano Letters* **2008**, *8*, 689.
[8] S. De, T. Higgins, P. E. Lyons, E. M. Doherty, P. N. Nirmalraj, W. J. Blau, J. J. Boland, J. N. Coleman, *ACS Nano* **2009**, *3*, 1767.
[9] C. M. Aguirre, S. Auvray, S. Pigeon, R. Izquierdo, P. Desjardins, R. Martel, *Applied Physics Letters* **2006**, *88*, 183104
[10] E. Artukovic, M. Kaempgen, D. S. Hecht, S. Roth, G. GrUner, *Nano Letters* **2005**, *5*, 757.
[11] T. M. Barnes, J. V. de Lagemaat, D. Levi, G. Rumbles, T. J. Coutts, C. L. Weeks, D. A. Britz, I. Levitsky, J. Peltola, P. Glatkowski, *Physical Review B* **2007**, *75*, 235410.
[12] T. M. Barnes, X. Wu, J. Zhou, A. Duda, J. van de Lagemaat, T. J. Coutts, C. L. Weeks, D. A. Britz, P. Glatkowski, *Applied Physics Letters* **2007**, *90*, 243503.
[13] M. A. Contreras, T. Barnes, J. van de Lagemaat, G. Rumbles, T. J. Coutts, C. Weeks, P. Glatkowski, I. Levitsky, J. Peltola, D. A. Britz, *Journal of Physical Chemistry C* **2007**, *111*, 14045.
[14] H. Z. Geng, K. K. Kim, K. P. So, Y. S. Lee, Y. Chang, Y. H. Lee, *Journal of the American Chemical Society* **2007**, *129*, 7758.
[15] H. Z. Geng, D. S. Lee, K. K. Kim, G. H. Han, H. K. Park, Y. H. Lee, *Chemical Physics Letters* **2008**, *455*, 275.
[16] G. Gruner, *Journal of Materials Chemistry* **2006**, *16*, 3533.
[17] M. Kaempgen, G. S. Duesberg, S. Roth, *Applied Surface Science* **2005**, *252*, 425.
[18] B. B. Parekh, G. Fanchini, G. Eda, M. Chhowalla, *Applied Physics Letters* **2007**, *90*, 121913.
[19] Z. C. Wu, Z. H. Chen, X. Du, J. M. Logan, J. Sippel, M. Nikolou, K. Kamaras, J. R. Reynolds, D. B. Tanner, A. F. Hebard, A. G. Rinzler, *Science* **2004**, *305*, 1273.
[20] A. K. Geim, K. S. Novoselov, *Nature Materials* **2007**, *6*, 183.
[21] S. Stankovich, D. A. Dikin, R. D. Piner, K. A. Kohlhaas, A. Kleinhammes, Y. Jia, Y. Wu, S. T. Nguyen, R. S. Ruoff, *Carbon* **2007**, *45*, 1558.
[22] S. Stankovich, D. A. Dikin, G. H. B. Dommett, K. M. Kohlhaas, E. J. Zimney, E. A. Stach, R. D. Piner, S. T. Nguyen, R. S. Ruoff, *Nature* **2006**, *442*, 282.
[23] D. A. Dikin, S. Stankovich, E. J. Zimney, R. D. Piner, G. H. B. Dommett, G. Evmenenko, S. T. Nguyen, R. S. Ruoff, *Nature* **2007**, *448*, 457.
[24] X. L. Li, G. Y. Zhang, X. D. Bai, X. M. Sun, X. R. Wang, E. Wang, H. J. Dai, *Nature Nanotechnology* **2008**, *3*, 538.
[25] S. Park, J. H. An, I. W. Jung, R. D. Piner, S. J. An, X. S. Li, A. Velamakanni, R. S. Ruoff, *Nano Letters* **2009**, *9*, 1593.
[26] G. Eda, G. Fanchini, M. Chhowalla, *Nature Nanotechnology* **2008**, *3*, 270.

[27] H. A. Becerril, J. Mao, Z. Liu, R. M. Stoltenberg, Z. Bao, Y. Chen, *Acs Nano* **2008**, *2*, 463.
[28] G. Eda, Y. Y. Lin, S. Miller, C. W. Chen, W. F. Su, M. Chhowalla, *Applied Physics Letters* **2008**, *92*, 233305.
[29] X. Wang, L. J. Zhi, K. Mullen, *Nano Letters* **2008**, *8*, 323.
[30] J. B. Wu, H. A. Becerril, Z. N. Bao, Z. F. Liu, Y. S. Chen, P. Peumans, *Applied Physics Letters* **2008**, *92*, 263302.
[31] Y. Hernandez, V. Nicolosi, M. Lotya, F. M. Blighe, Z. Y. Sun, S. De, I. T. McGovern, B. Holland, M. Byrne, Y. K. Gun'ko, J. J. Boland, P. Niraj, G. Duesberg, S. Krishnamurthy, R. Goodhue, J. Hutchison, V. Scardaci, A. C. Ferrari, J. N. Coleman, *Nature Nanotechnology* **2008**, *3*, 563.
[32] P. Blake, P. D. Brimicombe, R. R. Nair, T. J. Booth, D. Jiang, F. Schedin, L. A. Ponomarenko, S. V. Morozov, H. F. Gleeson, E. W. Hill, A. K. Geim, K. S. Novoselov, *Nano Letters* **2008**, *8*, 1704.
[33] M. Lotya, Y. Hernandez, P. J. King, R. J. Smith, V. Nicolosi, L. S. Karlsson, F. M. Blighe, S. De, Z. M. Wang, I. T. McGovern, G. S. Duesberg, J. N. Coleman, *Journal of the American Chemical Society* **2009**, *131*, 3611.
[34] T. Hertel, A. Hagen, V. Talalaev, K. Arnold, F. Hennrich, M. Kappes, S. Rosenthal, J. McBride, H. Ulbricht, E. Flahaut, *Nano Letters* **2005**, *5*, 511.
[35] Z. Sun, V. Nicolosi, D. Rickard, S. D. Bergin, D. Aherne, J. N. Coleman, *Journal of Physical Chemistry C* **2008**, *112*, 10692.
[36] L. M. Malard, M. A. Pimenta, G. Dresselhaus, M. S. Dresselhaus, *Physics Reports-Review Section of Physics Letters* **2009**, *473*, 51.
[37] A. C. Ferrari, J. C. Meyer, V. Scardaci, C. Casiraghi, M. Lazzeri, F. Mauri, S. Piscanec, D. Jiang, K. S. Novoselov, S. Roth, A. K. Geim, *Physical Review Letters* **2006**, *97*, 187401.
[38] L. Hu, D. S. Hecht, G. Gruner, *Nano Letters* **2004**, *4*, 2513.
[39] M. Dressel, G. Gruner, *Electrodynamics of Solids: Optical Properties of Electrons in Matter*, Cambridge University Press, Cambridge **2002**.
[40] R. R. Nair, P. Blake, A. N. Grigorenko, K. S. Novoselov, T. J. Booth, T. Stauber, N. M. R. Peres, A. K. Geim, *Science* **2008**, *320*, 1308.
[41] S. Park, R. S. Ruoff, *Nat Nano* **2009**, *4*, 217.

**TOC**

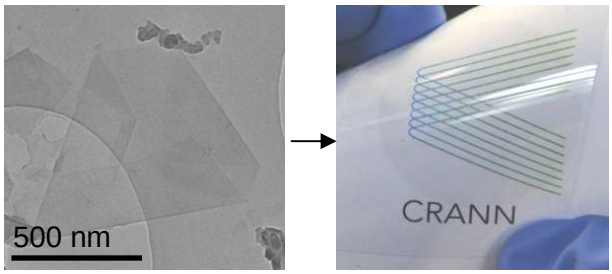


**Graphene thin films** are prepared using surfactant stabilized dispersions of graphene in water. Electromechanical stability coupled with high transparency make these films attractive as transparent flexible conductors.